Article

Experimental Investigation of Pulse Detonation Combustion Characteristics via Atomizer Geometry

Yoojin Oh [1], Myeung Hwan Choi [2] and Sungwoo Park [1,*]

1 Department of Smart Air Mobility, Korea Aerospace University, Goyang 10540, Republic of Korea; wlsdb34@naver.com
2 BK21 FOUR Smart Drone Convergence, Korea Aerospace University, Goyang 10540, Republic of Korea; nuclearreaction@hanmail.net
* Correspondence: sungwoo.park@kau.ac.kr

Abstract: Recent studies have increasingly focused on integrating detonation processes into engine technologies, advancing beyond the fundamental research phase of detonation research. The present study investigates the detonability and combustion characteristics of liquid fuels, specifically ethanol, with an emphasis on the effects of atomization properties facilitated by different atomizer designs to implement pulse detonation combustion engines. Oxygen was used as the oxidizer. We employed internal injectors (I45, I90, IB4) and atomizer venturis (VA, VB, VR) to examine how variations in liquid fuel atomization and atomizer configurations influence detonation. The occurrence of detonation was assessed using predicted Sauter mean diameters (SMDs) and exit velocities for different atomizer setups. Additionally, we evaluated the effects of nitrogen dilution at concentrations of 0%, 25%, and 50% on velocity variations and changes in detonation characteristics. The findings suggest that while higher exit velocities decrease SMD, facilitating detonation, excessively high velocities hinder detonation initiation. Conversely, lower exit velocities emphasize the role of SMD in initiating detonation. However, the introduction of nitrogen, which reduces the SMD, was found to decrease reactivity and impede detonation.

Keywords: atomizer; detonability; detonation; Sauter mean diameter; liquid fuel

1. Introduction

Detonation, a supersonic combustion process generating shockwaves, contrasts with deflagration, where the fuel–oxidizer mixture burns subsonically. Detonation, unlike subsonic deflagration, arises from either strong ignition or through the process of a deflagration encountering obstacles and transitioning to a supersonic combustion wave. Detonation engines operate based on the Fickett–Jacobs thermodynamic cycle, characterized by a rapid pressure rise during combustion, which contributes to these engines' high combustion efficiency [1]. The promising potential of detonation has fueled extensive research efforts exploring its application in gas turbines [2–4] and rocket engines [5,6]. Early detonation research focused on the fundamental aspects, including understanding Deflagration-to-Detonation Transition (DDT) devices [7–11], minimum ignition energy requirements [12–16], minimum tube diameters [17], and the characterization of detonation cells [18–24].

Building upon these fundamental studies, research has recently shifted towards detonation-based engines. Pulse Detonation Engines (PDEs) offer a simplified design concept, generating thrust through repetitive detonations occurring within a combustor, similar to the intake–compression–combustion–exhaust cycle of reciprocating engines. However, unlike pistons, PDEs utilize pressure waves generated by detonation for both combustion and exhaust. Therefore, PDEs with valves require careful optimization of fuel injection and purging. Valveless systems, while simpler in design, necessitate design optimization to ensure the mixer and combustion cycles are synchronized. Efforts are ongoing

to address these limitations by developing Rotating Detonation Engines (RDEs) [25–29]. RDEs achieve a significant overlap of detonation waves through lateral detonation initiation, eliminating the need for valves. This continuous detonation process makes them a promising candidate for propulsion systems. Previous studies have investigated the effect of injector geometry and conditions on detonation engine performance. Koo et al. [30] experimentally compared injectors with rectangular holes and slit-type injectors in a rotating detonation engine using gaseous oxygen and ethylene. They found that the injector with rectangular holes achieved more stable detonation and higher thrust. Shi et al. [31] performed a numerical study on how different injection conditions affect RDE characteristics. Their results showed that the area ratio between the head-end wall and the injector has a significant effect on thrust output.

In the initial stages of detonation engine research, gaseous fuels were favored because of their higher reactivity compared to liquid fuels. This higher reactivity facilitates easier initiation of detonation, resulting in quicker reaction times and more efficient purging of reactants during the fuel injection process. However, for practical applications such as use in propulsion systems, liquid fuels are favored due to their advantages in regard to storage and handling. Consequently, research into the use of liquid fuels in detonation engines is actively being conducted [32–35]. Wang et al. [32] investigated the impact of ignition energy on PDE performance using gasoline and kerosene. They found that increasing ignition energy resulted in shorter detonation initiation times and higher average thrust. Fan et al. [33] conducted experiments with a liquid octene (C_8H_{16}) and air in a PDE. They tested combustion chambers of different lengths and diameters. Their results showed that a chamber with a length of 1 m and a diameter of 50 mm achieved detonation combustion at a frequency of 36 Hz. Li et al. [34] successfully achieved detonation in a PDE using Jet A-1 fuel and air injected at around 70 °C. They found that a two-phase mixture at stoichiometric or slightly richer equivalence ratios facilitated detonation initiation more readily. Tan et al. [35] investigated the influence of air temperature on detonation characteristics in a PDE fueled by gasoline and air. They observed a decrease in the DDT distance with increasing air temperature. Detonation in liquid-fueled engines requires small droplets for efficient mixing with the oxidizer. These small droplets, with high evaporation rates, behave more like gases and enhance detonability. Therefore, research on atomizer design for the proper atomization of liquid fuels is crucial for achieving detonation in these engines. Gubin and Sichel [36] reported that a droplet size below 20 μm is necessary to achieve a detonation velocity close to the Chapman–Jouguet (CJ) detonation velocity, while successful propagation of cylindrical detonations has been achieved using fuels like decane, kerosene, and heptane with a larger SMD of around 400 μm [37]. Similar to the present study, Kadosh and Michaels [38] achieved detonation using ethanol and oxygen with an SMD of 30 μm.

Recent research on liquid-fueled detonation engines includes experiments on rotating detonation conducted by Li et al. [39]. This study investigated the feasibility of using Jet A-1 fuel in both premixed and non-premixed configurations within an RDE. They successfully achieved detonation in both scenarios. However, for the non-premixed case, the Jet A-1 fuel was finely atomized, generating an aerosol state that behaved very similarly to a gas for improved mixing with the oxidizer. Choi et al. [40] conducted spray experiments to investigate the influence of atomizer geometry on liquid fuel atomization. They varied the diameter of the venturi nozzle (relative to the injector diameter) at two different ratios ($R_e/R_i = 0.3, 1.0$) and used four different internal injector types (A–D). By analyzing spray images, they estimated the liquid film length and measured the Sauter mean diameter (SMD) of the droplets. This allowed them to develop an empirical formula to predict the SMD for each specific atomizer and venturi nozzle combination. Essentially, they aimed to predict droplet size based on the atomizer's geometry to anticipate its impact on detonability in future experiments. Their results showed that the venturi nozzle with $R_e/R_i = 0.3$ exhibited consistent spray characteristics regardless of the injector type, suggesting an air-assist atomization mechanism. In contrast, the venturi with $R_e/R_i = 1.0$ relied on an air-blast mechanism, leading to variations in spray characteristics depending on the

injector type. This finding highlights that the venturi nozzle's design has a more significant influence on the resulting spray properties than the internal fuel injector type.

The present study aimed to develop a novel valveless liquid detonation engine and determine how the geometry of the internal injector and venturi nozzle affects the degree of atomization, ultimately influencing detonability.

2. Experimental Setup

2.1. Pulse Detonation Combustion System

A schematic of the combustion chamber is depicted in Figure 1, with a chamber length of 806.5 mm. Four orifices were installed in the combustion chamber at intervals of 137.4 mm to facilitate the Deflagration-to-Detonation Transition (DDT). In order to promote turbulence generation within the relatively short combustion chamber, the Blockage Ratio (BR) was set to 0.8. Pressure transducers were installed at x/D = 10, 16, 21, and 27 to measure velocity and pressure changes between orifices. The control of the solenoid valve for propellant supply was achieved using an Arduino module. To generate 10 Hz pulse detonation, a valveless system that does not require valve opening and closing within the sequence was adopted. As shown in Figure 2, ignition was applied for 20 ms after 80 ms of supplying propellant. Ethanol is an attractive renewable fuel for automotive and power generation applications. It is a liquid at room temperature and has a relatively high vapor pressure, allowing it to be easily vaporized. Therefore, ethanol was chosen as the fuel to be employed, with oxygen serving as the oxidizer. To investigate the effect of exit velocity SMD at a constant equivalence ratio, experiments were conducted with the addition of nitrogen at 25% and 50%. The experiments were carried out at atmospheric pressure and room temperature. The oxygen supply pressure was set to 2 MPa, while the nitrogen supply pressure was set to 16 MPa.

Ethanol was supplied using a metering valve to control the mass flow at 0.4, 0.6, 0.8, and 1 g/s, while oxygen was fixed at 3.9 g/s. Nitrogen was controlled using a mass flow controller (Bronkhorst mini CORI-Flow meter), providing mass flows of 0, 1.2, and 3.7 g/s. The flow meters have a range from 2 kg/h to 100 kg/h, with an accuracy of ±0.2%. The installed pressure transducer was a PCB Piezotronics 113B24 model with a sensitivity of 755.1 mV/MPa and an uncertainty of ±1.0%. The signal measured by the pressure transducer is converted through a signal conditioner (PCB Piezotronics 482C Series) and then stored on a computer using LabVIEW software. To capture detonation waves, data were collected at a rate of 110 kHz.
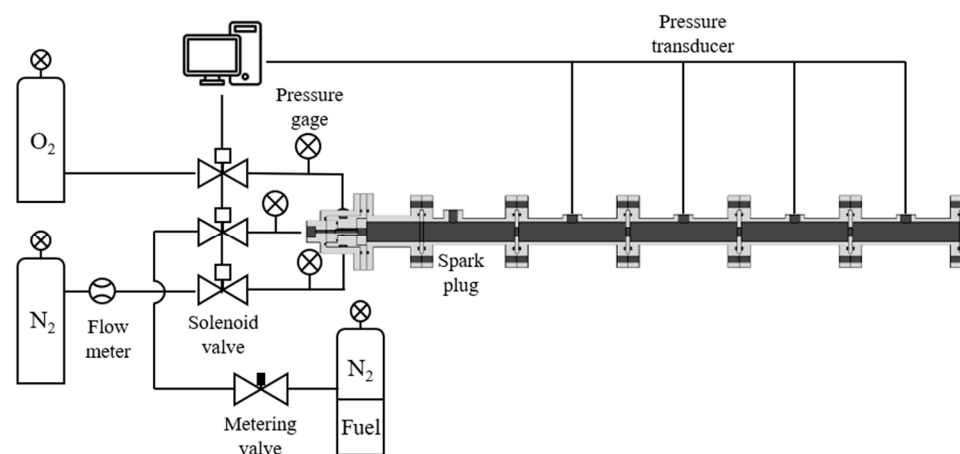

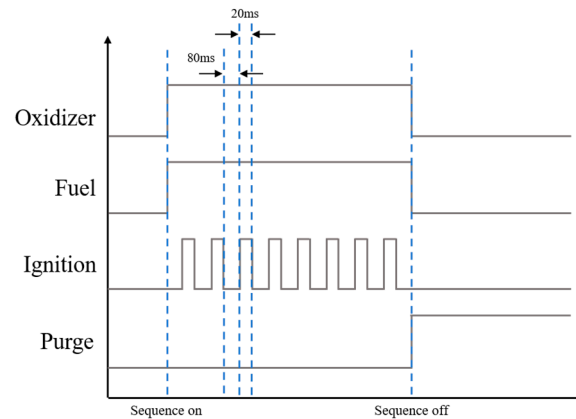**Figure 1.** Schematic of pulse detonation combustion system.

Figure 2. Sequence for valveless system (10 Hz).

2.2. Atomizer

Figure 3 displays the atomizer designed based on the research conducted by Yan et al. [41]. Injectors I45, I90, and IB4 were designed to vary the direction and position of the internal liquid fuel, while venturis VA, VB, and VR were designed to determine the exit shape of the atomizer. The fuel injection holes for I45, I90, and IB4 each have four fuel spray holes, each with a diameter of 0.5 mm. Spray holes measuring 0.5 mm are located at the same position for I45 and I90, while for IB4, they are positioned 10 mm behind the end of the injector. I45 has an angled end of 45 degrees, causing ethanol to be sprayed diagonally, whereas I90 and IB4 spray ethanol vertically. This study investigates the impact of injector geometry on detonation characteristics in a liquid-fueled PDE. Specifically, we compared and analyzed detonation based on the variations in momentum ratio and spray angle for injectors I45 and I90. Additionally, the influence of the gap between the injector tip and the fuel hole upon detonation was examined using injector IB4.
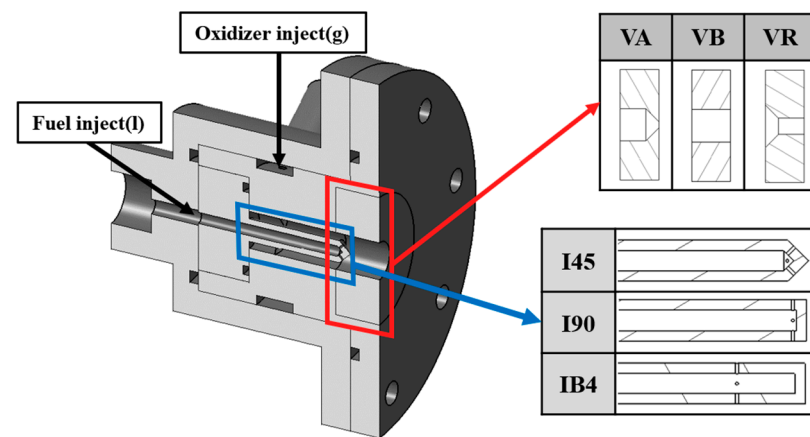

Figure 3. Schematic of atomizer.

The atomizer operates as a two-phase atomizer, using the momentum of the oxidizer to atomize the liquid. Following previous research conducted by Choi et al. [40], the VA venturi, with a diameter of 3 mm, functions as an air-assist type atomizer by achieving a high exit velocity to atomize the liquid. In contrast, the VB venturi demonstrates spray characteristics similar to those of an air-blast-type atomizer, with relatively lower velocity and higher airflow rates for liquid atomization. It has been found that the nozzle area of the venturi exit has a significantly greater influence on atomization performance compared to the shape of the injector. Therefore, variables related to the shape of the injector were excluded in these combustion experiments. In addition, a VR venturi with a recess was included in this experiment to assess the effect of the recess. The injectors used in these

detonation experiments are shown in Figure 4. For the VB venturi, all injectors (I45, I90, IB4) were tested, while for the VA and VR venturis, only the I45 injector was tested because it was observed that the injectors exerted minimal influence.
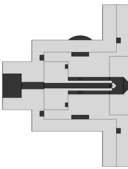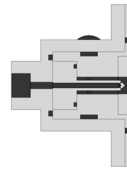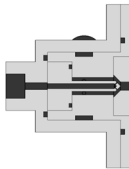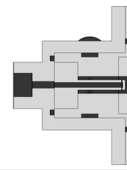

Figure 4. Types of atomizers used in detonation experiments.

The VR venturi is described in detail in Figure 5. Its exit diameter is 5 mm, and the recess length is 8 mm. Furthermore, research on detonability was conducted using the SMD empirical equations proposed by Choi et al. (Equations (1) and (2)) [40]. The SMD of the VR venturi was estimated using the empirical equation for the VB ($R_e/R_i = 1.0$) venturi. As shown in Figure 6, the high correlation ($R^2 = 0.84$) indicates a strong relationship, allowing for the estimation of the VR venturi's SMD through the VB venturi equation.

$$\frac{SMD}{d_0} = 5.91 \times Re_{e,g}^{-0.55} \, We_l^{-0.06} \, q^{-0.31} \left(\frac{L_g}{L_l} \right)^{0.01} \tag{1}$$

$$\frac{SMD}{d_0} = 3.03 \times Re_{e,g}^{-0.46} \, We_l^{-0.17} \, q^{-0.35} \left(\frac{L_g}{L_l} \right)^{0.12} \tag{2}$$
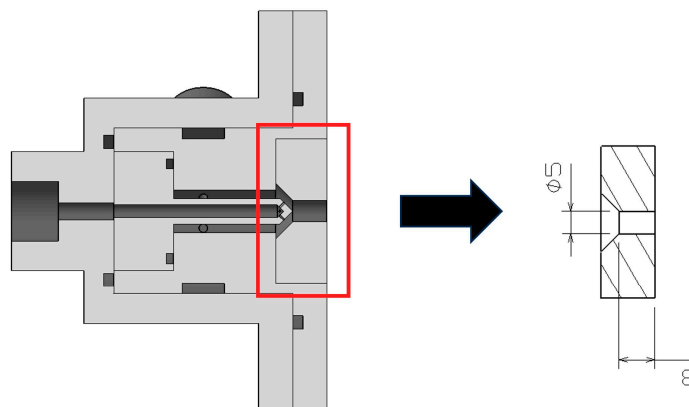

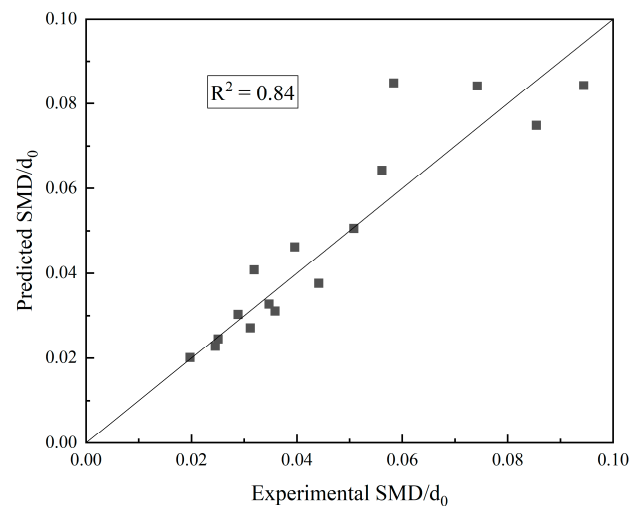**Figure 5.** Schematic of VR venturi.

Figure 6. Correlation between experimental SMD and predicted SMD.

3. Results

3.1. Detonation Characteristics with N_2 Dilution and Equivalence Ratio

The VA and VB venturis achieved detonation at frequencies up to 6 Hz, while the VR venturi reached detonation at up to 15 Hz. Figure 7 presents pressure data acquired at 10 Hz using a VR venturi. The data show there was no significant decrease in von Neumann spike pressure over time. The sustainability of pulse detonation is determined by the complex interplay of various factors, such as the shape of the venturi nozzle outlet, injector configuration, the equivalence ratio, and the amount of nitrogen added. Some pulse detonation experiments encountered issues like flames attaching to the combustion chamber walls or combustion instability. In the case of the VB venturi nozzle, where flame formation occurred inside the venturi nozzle, the insufficient cooling of the combustion chamber resulted in the destruction of the injector, as shown in Figure 8. This destruction can occur due to a low oxidizer velocity when the outlet area of the venturi nozzle is large.

Figures 9 and 10 illustrate the relationship between detonation occurrence, the equivalence ratio, and nitrogen dilution. For the VB venturi, injectors I45 and I90 exhibited similar detonation tendencies across all the tested conditions (concerning the equivalence ratio and nitrogen dilution). However, injector IB4 behaved differently, failing to achieve detonation under the same conditions. This was attributed to two factors: the larger SMD of the IB4 injector and the location of its fuel injection hole. These factors increased the likelihood of flame attachment within the atomizer. Consequently, injector IB4 suffered more frequent damage.
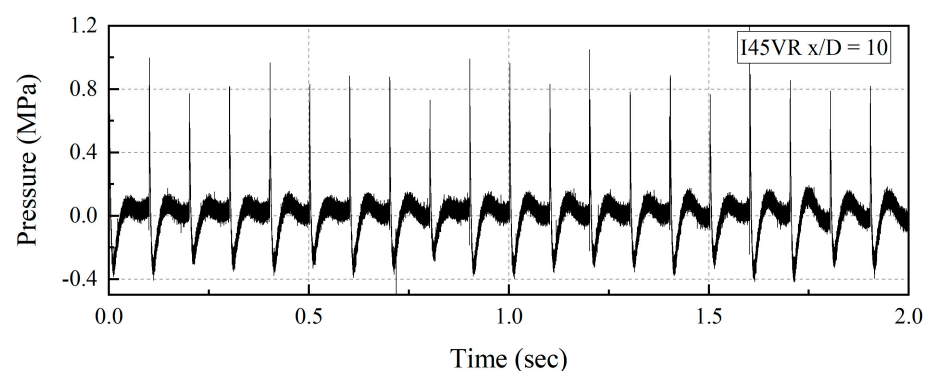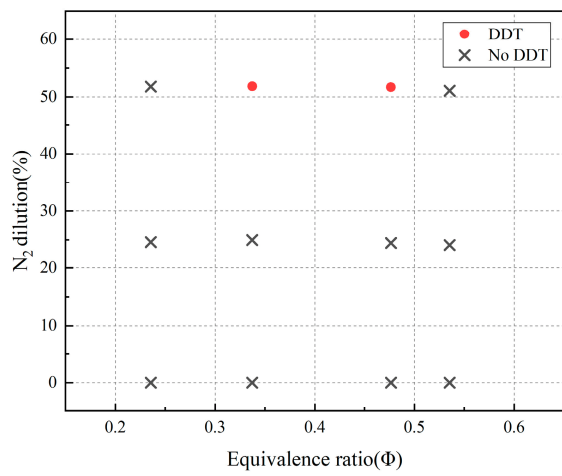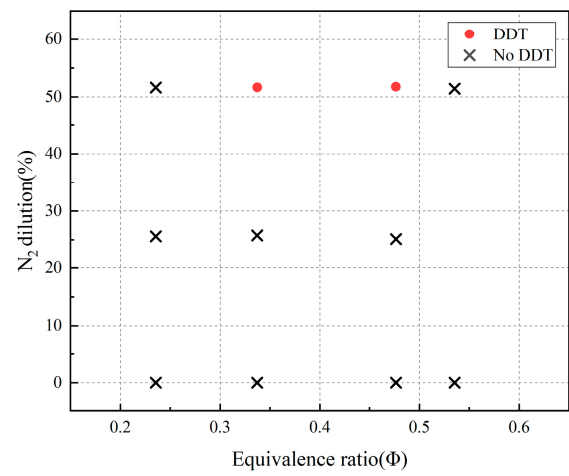

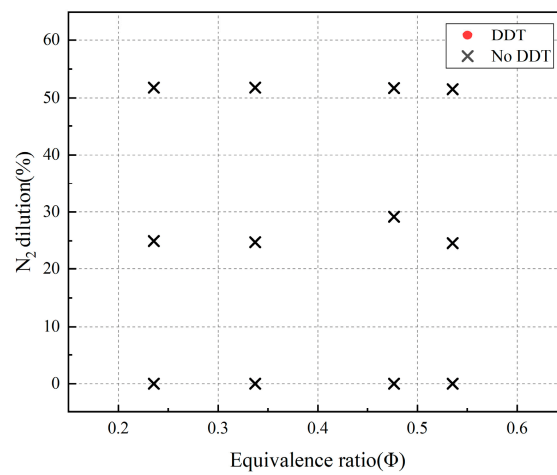**Figure 7.** The pressure at x/D = 10 of I45VR injector.

Figure 8. Injector failure caused by flame formation in the VB venturi.

(**a**)

(**b**)

(**c**)

Figure 9. Influence of equivalence ratio and nitrogen dilution on detonation transition: (**a**) I45VB; (**b**) I90VB; (**c**) IB4VB.
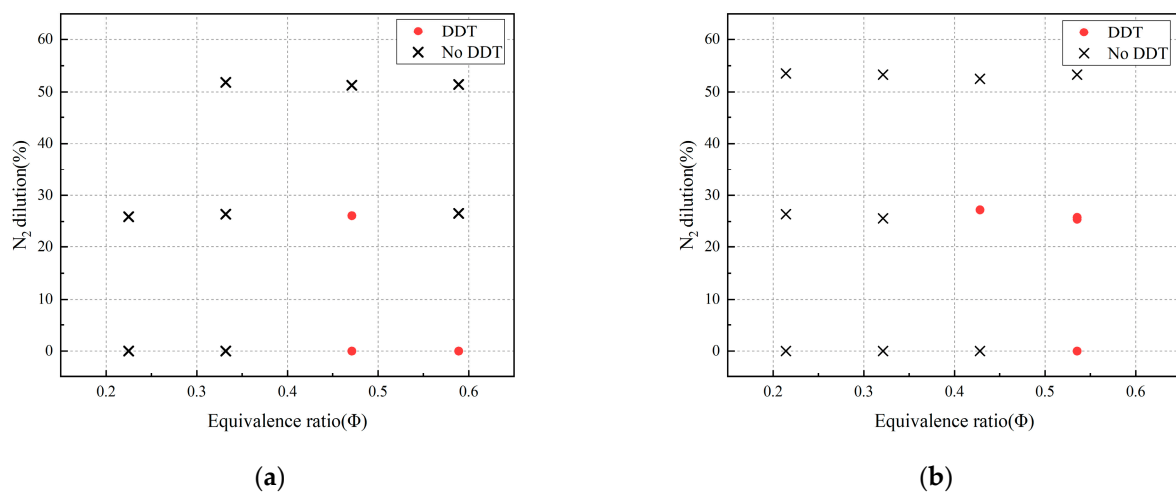
Figure 10. Influence of equivalence ratio and nitrogen dilution on detonation transition: (**a**) I45VA; (**b**) I45VR.

The results also indicate that the venturi diameter interacts with the effect of nitrogen upon detonation. For the smaller diameter VA venturi, the high exit velocity promotes adequate fuel atomization even without nitrogen dilution. Consequently, the introduction of nitrogen hinders detonation by reducing the overall reactivity of the mixture. Conversely, the larger 10 mm diameter of the VB venturi leads to a lower exit velocity, hindering atomization. In this case, including nitrogen at 50% enhances fuel atomization at the higher velocity, promoting detonation transition. The VR venturi acts as an intermediate between VA and VB. Its design allows detonation at an appropriate velocity without requiring a specific nitrogen concentration (around 25% for VR).

3.2. Detonation Characteristics with Respect to SMD and Venturi Exit Velocity

Based on previous studies [40], the SMD in the detonation combustion experiments was estimated using the SMD empirical Equations (1) and (2). This approach underscores the relationship between the oxidizer velocity at the injector and the resulting droplet size. This method was used to predict the combustion characteristics of liquid fuel injected inside high-temperature and high-pressure chambers using a database developed from the results of atomizer tests conducted under room-temperature and atmospheric pressure conditions.

Figure 11 shows the predicted SMD for the VA venturi's oxidizer exit velocities. Different nitrogen dilutions are represented by different colors, and instances where detonation occurred are marked with circular symbols. The VA venturi's relatively narrow nozzle outlet leads to inherently high exit velocities, typically exceeding 120 m/s, and a very small SMD ranging from 6 to 11 μm. In the VA venturi, increasing the mass flow rate modestly increases the velocity near the injector. However, the most significant effect is a pressure increase around the internal injector due to the venturi effect caused by the narrow nozzle outlet area. Detonation occurred when the velocity near the venturi exit was below 150 m/s, as seen in region I, with an SMD of around 10 μm. At this size, droplets rapidly evaporate, behaving similarly to gases in terms of reactivity. Conversely, when detonation failed to occur despite SMDs being below 10 μm in region II, the dominant factor appeared to be the exit velocity near the venturi nozzle. Velocities exceeding 150 m/s likely disrupt the initial propellant ignition, hindering a sustained reaction even if it starts.
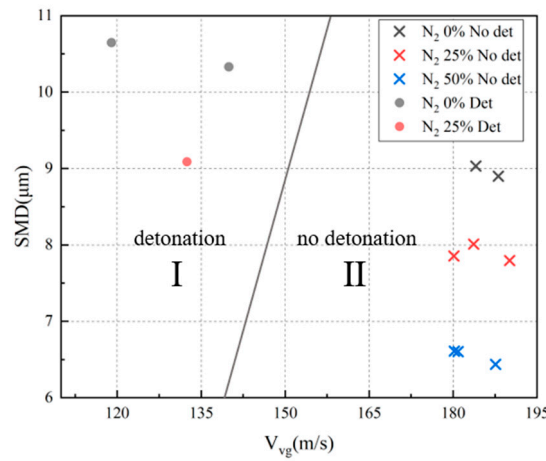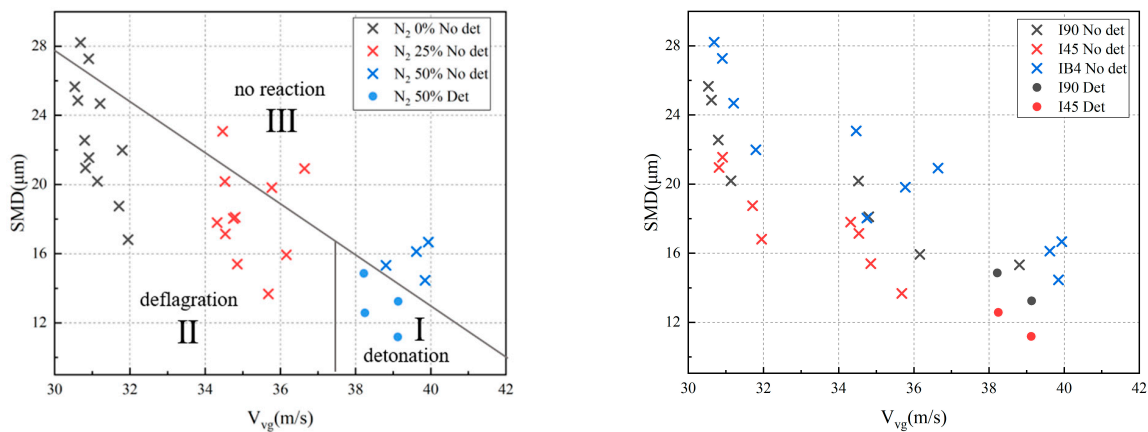
Figure 11. SMD as a function of exit velocity of the VA venturi.

Figure 12 displays the distinct characteristics of the VB venturi compared to the VA. Unlike the VA venturi, with its high exit velocities, the VB venturi exhibits a relatively low velocity, typically less than 42 m/s. This behavior is characteristic of air-blast atomizers, where the shape of the injector inside the atomizer and the momentum ratio between air and fuel become important factors for atomization, unlike the VA venturi, which depends primarily on a high exit velocity. As shown in Figure 12a, the addition of nitrogen increases the flow rate, which, in turn, raises the velocity, resulting in a smaller SMD. This highlights the importance of oxidizer flow rate in the atomization mechanism of the air-blast atomizer. In areas where detonation occurred, such as region I, nitrogen dilution reached 50%. This suggests that the decrease in SMD due to the higher exit velocity played a key role in facilitating the transition to detonation. As can be seen in region III, despite having a small SMD and falling within the reactive exit velocity range, detonation did not occur in some areas. This can be attributed to the high concentration of nitrogen, which hindered the transition to detonation. Figure 12b categorizes colors based on the types of internal injectors. Following the sequence of IB4, I90, and I45, there was a gradual decrease in SMD, with variations in injector types revealing a difference of up to 8 μm in the SMD. In a previous study [40], it was found that the SMD of the I45 injector was smaller than that of the I90 injector at high fuel mass flow rates. This difference was attributed not only to the air-blast atomization mechanism but also to complex factors including the length of the liquid film. Furthermore, it was suggested that despite a small difference in SMD, the venturi's impact is more significant than that of internal injectors.

(**a**) N₂ dilution effect

(**b**) Injector type

Figure 12. SMD as a function of exit velocity for the VB venturi.

However, combustion experiments revealed that IB4 suffered from significant cooling problems. As illustrated in Figure 8, this resulted in flame attachment within the chamber, which caused injector melting. This phenomenon appears to be linked to the combination of the larger SMD and the recessed fuel holes, leading to internal flame attachment, unlike what occurs in other injectors.

Figure 13 shows that the VR venturi exhibits an intermediate trend for both SMD and exit velocity compared to VA and VB. As the nitrogen concentration is diluted, the exit velocity increases, which, in turn, leads to a decrease in SMD. However, as observed in region II, a high nitrogen concentration inhibits detonation. The SMD is important because it reflects how quickly fuel evaporates, reacts with the oxidizer, and then rapidly extinguishes the flame to prepare for the subsequent explosion. Therefore, maintaining the SMD below a certain threshold is critical for detonation. The atomization mechanism necessitates high velocities to achieve a lower SMD, but these high velocities can disrupt the mixing process, preventing an effective reaction between the fuel and oxidizer. Finding a balance between attaining a small SMD and maintaining optimal mixing conditions is essential for the efficient operation of pulse detonation engines.
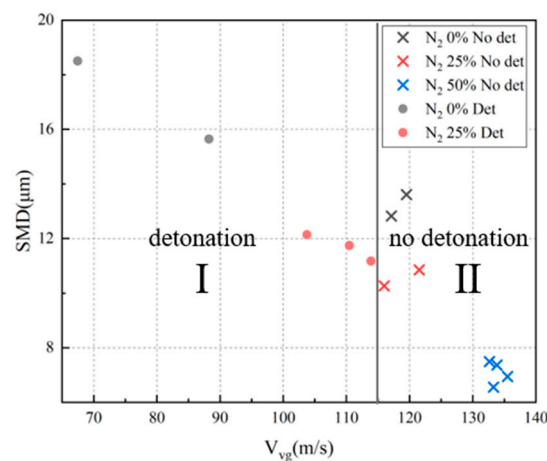

Figure 13. SMD as a function of exit velocity for the VR venturi.

3.3. Detonation Pressure and Velocity Characteristics with x/D

The von Neumann spike is a key indicator of detonation intensity. It consists of the sharp rise in pressure caused by the overlapping shockwaves that precede the reaction zone in the detonating propellant mixture. After the spike, the chemical reaction within the mixture ignites and progresses until reaching the Chapman–Jouguet (C-J) point. Higher reaction rates of the fuel–oxidizer mixture or explosive lead to faster overlap of the shockwaves, resulting in a stronger pressure spike. Conversely, slower reaction rates lead to weaker overlap and a diminished spike magnitude.

Figure 14a illustrates the maximum pressure based on the type of Venturi nozzle and the measurement location. Generally, for all Venturi nozzle types, positions nearer to the injector, with a lower x/D ratio, tend to show higher von Neumann spikes. This is because the initial pressure measurement point is closest to the spark plug, where the high ignition energy has a significant impact. As the x/D ratio increases, the pressure from the shockwave diminishes due to the combustor being open on one side, which leads to a sharp decrease in the von Neumann spike toward the rear of the combustor. Among the Venturi nozzle types, the VA Venturi exhibits the highest von Neumann spike, followed by VR and VB, in that order. Interestingly, the von Neumann spike pressure of the VB Venturi becomes higher than the pressures of the VA and VR at the x/D = 27 position. This observation indicates that the Venturi exit geometry significantly influences the maintenance of the von Neumann spike pressure.
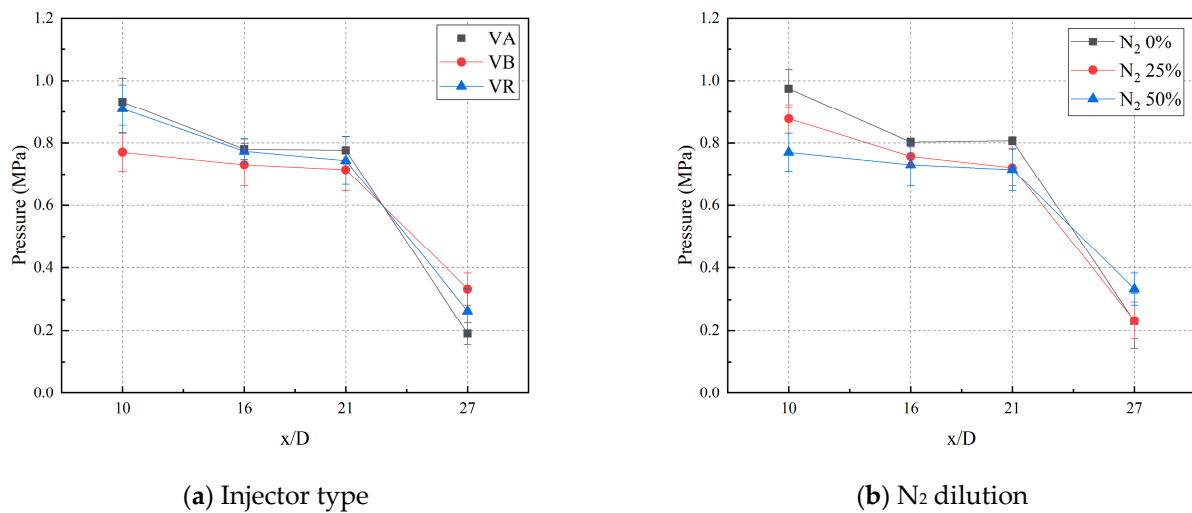
(**a**) Injector type   (**b**) N_2 dilution

Figure 14. von Neumann spike pressure variation as a function of x/D ($\Phi = 0.32 - 0.58$).

Figure 14b represents the maximum pressure as a function of nitrogen dilution in the oxidizer, independent of the venturi nozzle type. Increasing nitrogen dilution in the oxidizer leads to a decrease in the maximum pressure of the von Neumann spike. This is because the added nitrogen chemically reduces the reaction rate of the fuel–oxidizer mixture within the combustor. While nitrogen dilution can enhance the velocity of exit from the venturi nozzle and promote finer atomization (smaller droplets), leading to faster mixing, it also acts as a chemical inhibitor that lowers the overall reaction rate. This can hinder the initiation and intensity of detonation in the combustor.

V_{exp}/V_{CJ} is the detonation velocity ratio, defined as the experimentally measured velocity divided by the theoretical Chapman–Jouguet (C-J) velocity. A value of V_{exp}/V_{CJ} approaching unity indicates that the measured velocity is close to the theoretical C-J velocity. The C-J velocity represents a detonation wave where the reaction zone and the shockwave are perfectly coupled. In this state, the reaction products exiting the detonation wave achieve a sonic velocity relative to the unreacted material. Due to this coupling, the C-J velocity is a valuable theoretical tool for predicting detonation characteristics in various explosive materials [42,43]. The C-J velocity was determined using NASA's CEA code [44]. The detonation velocity was measured using the Time-of-Flight (TOF) method [45]. In this method, velocity is calculated by dividing the distance between two pressure transducers by the time difference between the arrival of the detonation wave's arrival at each sensor.

Figure 15a illustrates the variation in V_{exp}/V_{CJ} with respect to x/D for different venturi nozzle types. V_{exp}/V_{CJ} generally increases upon increasing x/D, reaching a peak value around x/D = 18.5. This suggests an acceleration of the deflagration wave due to the progressive overlap of shockwaves as it propagates further downstream (higher x/D) through the DDT orifice. Beyond x/D = 18.5, the V value decreases, indicating that the detonation wave ceases to accelerate.

Consistent with Figure 14a, the V_{exp}/V_{CJ} values are generally highest for the VA nozzle, followed by those for the VR and then VB nozzles. This trend aligns with the higher von Neumann spike pressures observed for the VA nozzle in Figure 14a. The correlation between V_{exp}/V_{CJ} and von Neumann spike pressure at lower x/D (at which point the reaction initiates) suggests a potential influence of the atomization mechanism or the distribution of SMDs at the venturi exit on the initial detonation velocity. Figure 15b shows the effect of nitrogen dilution on the relationship between x/D and V_{exp}/V_{CJ}. At low x/D values (before the DDT), the V_{exp}/V_{CJ} is significantly lower when nitrogen dilution is present. This suggests that nitrogen addition weakens the initial stages of the detonation. When nitrogen is present, passing through the DDT orifice leads to a greater increase in the V_{exp}/V_{CJ} compared to cases without dilution. Figures 14b and 15b also show that the von Neumann spike pressure and V_{exp}/V_{CJ} for the case with 50% N_2 dilution are close to

those of the undiluted case at the largest x/D. This suggests that nitrogen may enhance turbulence, thereby improving the efficiency of the DDT device and contributing to the maintenance of the detonation wave. This effect becomes more pronounced with higher nitrogen dilution levels. This implies that the DDT orifice plays a more critical role in accelerating the detonation wave when inert gases like nitrogen are introduced, potentially by enhancing mixing or shockwave interactions.
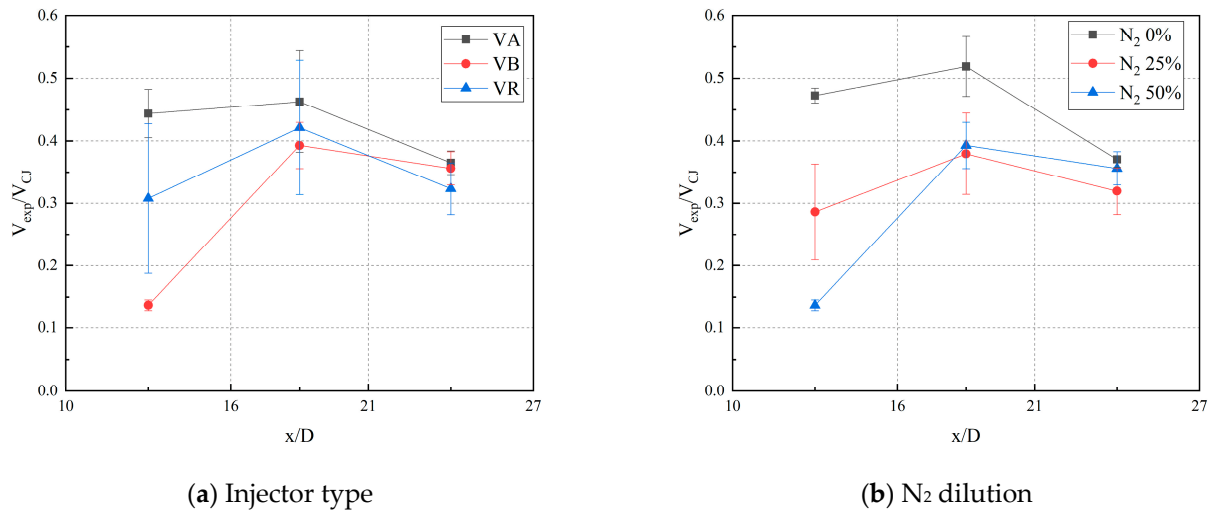

(**a**) Injector type   (**b**) N₂ dilution

Figure 15. V_{exp}/V_{CJ} as a function of x/D ($\Phi = 0.32 - 0.58$).

Overall, both the von Neumann spike pressure and the detonation velocity ratio are influenced by the venturi nozzle type and the level of nitrogen dilution in the oxidizer. The venturi nozzle type affects factors like the exit flow velocity and the resulting atomization of the fuel, which determines the SMD of the fuel droplets. Nitrogen dilution directly impacts the reactivity of the propellant mixture by reducing the concentrations of fuel and oxidizer.

4. Discussion and Conclusions

This study investigated the influence of injector and venturi geometry on detonability in a valveless liquid fuel detonation system. To achieve this, a system for liquid fuel detonation was designed and fabricated, including injectors and venturi nozzles for efficient fuel atomization. Pulse detonation with a two-phase injector requires a uniform fuel mixture with an SMD below a critical threshold when mixed with the oxidizer. Based on the prior research on the impact of injector and venturi geometry on spray characteristics, combustion experiments were conducted to identify the specific spray properties that influence detonability. A summary of the key findings is given below.

1. Increasing the venturi nozzle's exit velocity effectively reduces the SMD of the fuel droplets, as observed during the spraying process. This is a proper approach to achieving a uniform distribution of droplet sizes, which is significant for detonation. However, excessively high exit velocities can have a detrimental effect on detonability. Therefore, it is essential to find the optimal exit velocity that balances achieving a desired SMD with a high fuel evaporation rate to ensure optimal detonation efficiency.
2. At lower velocities of exit from the venturi nozzle, the impact of the SMD on achieving detonation becomes more important. The VB venturi, which functions similarly to an air-blast atomizer, is particularly effective at producing small SMDs even at these lower velocities. However, for high-frequency pulse detonation cycles, a very low SMD, ideally around 20 μm or below, is necessary.
3. Adding nitrogen to increase the exit velocity can reduce the SMD. However, from a reactivity standpoint, this addition can negatively affect detonation. Although adding nitrogen can result in a sufficiently small SMD with a high evaporation rate,

enhancing detonability, the introduction of nitrogen significantly reduces reactivity. Consequently, using gases with low reactivity, like nitrogen, in the atomizer to decrease the SMD may not be the best approach.

4. The addition of nitrogen can potentially enhance the acceleration of detonation waves through the DDT device compared to that occurring without the addition of nitrogen. This suggests that nitrogen dilution at an optimal ratio might be beneficial for accelerating detonation waves, provided a sufficiently low SMD is still achieved.

The results of this study can contribute to achieving high-frequency detonation with liquid fuels by identifying key factors influencing detonability based on injector and venturi nozzle geometry. These insights might contribute to the development of internal spraying methods for future Pulse Detonation Engine (PDE) designs.

Author Contributions: Conceptualization, M.H.C., Y.O., and S.P.; methodology, M.H.C., Y.O., and S.P.; software, M.H.C., Y.O., and S.P.; validation, M.H.C., Y.O., and S.P.; formal analysis, M.H.C., Y.O., and S.P.; investigation, M.H.C., Y.O., and S.P.; resources, M.H.C., Y.O., and S.P.; data curation, M.H.C., Y.O., and S.P.; writing—original draft preparation, M.H.C., Y.O., and S.P.; writing—review and editing, M.H.C., Y.O., and S.P.; visualization, M.H.C., Y.O., and S.P.; supervision, M.H.C., Y.O., and S.P.; project administration, M.H.C., Y.O., and S.P.; funding acquisition, M.H.C., Y.O., and S.P. All authors have read and agreed to the published version of the manuscript.

Data Availability Statement: The data supporting the findings of this study are available from the corresponding author upon reasonable request.

Conflicts of Interest: The authors declare no conflicts of interest.

References

1. Wintenberger, E.; Shepherd, J.E. Thermodynamic cycle analysis for propagating detonations. *J. Propuls. Power* **2006**, *22*, 694–698. [CrossRef]
2. Rasheed, A.; Furman, A.; Dean, A. Experimental investigations of an axial turbine driven by a multi-tube pulsed detonation combustor system. In Proceedings of the 41st AIAA/ASME/SAE/ASEE Joint Propulsion Conference & Exhibit, Tucson, AZ, USA, 10–13 July 2005; p. 4209.
3. Glaser, A.; Caldwell, N.; Gutmark, E. Performance of an axial flow turbine driven by multiple pulse detonation combustors. In Proceedings of the 45th AIAA Aerospace Sciences Meeting and Exhibit, Reno, Nevada, 8–11 January 2007; p. 1244.
4. Xisto, C.; Petit, O.; Grönstedt, T.; Rolt, A.; Lundbladh, A.; Paniagua, G. The efficiency of a pulsed detonation combustor–axial turbine integration. *Aerosp. Sci. Technol.* **2018**, *82*, 80–91. [CrossRef]
5. Sosa, J.; Berry, Z.; Burke, R.; Ahmed, K.A.; Micka, D. Exploration of nozzle flow circumferential attenuation and efficient expansion for rotating detonation rocket engines. In Proceedings of the AIAA Scitech 2020 Forum, Orlando, FL, USA, 6–10 January 2020; p. 0197.
6. Batista, A.; Ross, M.; Lietz, C.; Hargus, W.A. Descending modal transition study in a rotating detonation rocket engine. In Proceedings of the AIAA Scitech 2021 Forum, Online, 11–15 January 2021; p. 0191.
7. New, T.; Panicker, P.; Lu, F.; Tsai, H. Experimental investigations on DDT enhancements by Schelkin spirals in a PDE. In Proceedings of the 44th AIAA Aerospace Sciences Meeting and Exhibit, Reno, NV, USA, 9–12 January 2006; p. 552.
8. Cross, M.; Ciccarelli, G. DDT and detonation propagation limits in an obstacle filled tube. *J. Loss Prev. Process Ind.* **2015**, *36*, 380–386. [CrossRef]
9. Ciccarelli, G.; Wang, Z.; Lu, J.; Cross, M. Effect of orifice plate spacing on detonation propagation. *J. Loss Prev. Process Ind.* **2017**, *49*, 739–744. [CrossRef]
10. Sun, X.; Lu, S. Effect of obstacle thickness on the propagation mechanisms of a detonation wave. *Energy* **2020**, *198*, 117186. [CrossRef]
11. Ciccarelli, G.; Fowler, C.J.; Bardon, M. Effect of obstacle size and spacing on the initial stage of the flame acceleration in a rough tube. *Shock Waves* **2005**, *14*, 161–166. [CrossRef]
12. Sato, T.; Matsuoka, K.; Kawasaki, A.; Itouyama, N.; Watanabe, H. Experimental demonstration on detonation initiation by laser ignition and shock focusing in elliptical cavity. *Shock Waves* **2023**, *33*, 521–531. [CrossRef]

13. Zhang, B.; Ng, H.D.; Lee, J.H. Measurement of effective blast energy for direct initiation of spherical gaseous detonations from high-voltage spark discharge. *Shock Waves* **2012**, *22*, 1–7. [CrossRef]
14. Lefkowitz, J.K.; Guo, P.; Ombrello, T.; Won, S.H.; Stevens, C.A.; Hoke, J.L.; Schauer, F.; Ju, Y. Schlieren imaging and pulsed detonation engine testing of ignition by a nanosecond repetitively pulsed discharge. *Combust. Flame* **2015**, *162*, 2496–2507. [CrossRef]
15. Wang, Z.; Zhang, Y.; Huang, J.; Liang, Z.; Zheng, L.; Lu, J. Ignition method effect on detonation initiation characteristics in a pulse detonation engine. *Appl. Therm. Eng.* **2016**, *93*, 1–7. [CrossRef]
16. Zhang, B.; Chang, X.; Bai, C. End-wall ignition of methane-air mixtures under the effects of $CO_2/Ar/N_2$ fluidic jets. *Fuel* **2020**, *270*, 117485. [CrossRef]
17. Sun, X.; Yan, C.; Yan, Y.; Mi, X.; Lee, J.H.; Ng, H.D. Critical tube diameter for quasi-detonations. *Combust. Flame* **2022**, *244*, 112280. [CrossRef]
18. Ciccarelli, G.; Ginsberg, T.; Boccio, J.; Economos, C.; Sato, K.; Kinoshita, M. Detonation cell size measurements and predictions in hydrogen-air-steam mixtures at elevated temperatures. *Combust. Flame* **1994**, *99*, 212–220. [CrossRef]
19. Lee, J. The propagation mechanism of cellular detonation. In Proceedings of the Shock Waves: Proceedings of the 24th International Symposium on Shock Waves, Beijing, China, 11–16 July 2004; Springer: Berlin/Heidelberg, Germany, 2005; pp. 19–30.
20. Ciccarelli, G.; Cross, M. On the propagation mechanism of a detonation wave in a round tube with orifice plates. *Shock Waves* **2016**, *26*, 587–597. [CrossRef]
21. Kellenberger, M.; Ciccarelli, G. Simultaneous schlieren photography and soot foil in the study of detonation phenomena. *Exp. Fluids* **2017**, *58*, 138. [CrossRef]
22. Hageman, M.D.; Knadler, M. Detonation Cell Size of Methane with Nitrous Oxide. In Proceedings of the AIAA Propulsion and Energy 2020 Forum, Online, 24–28 August 2020; p. 3860.
23. Hageman, M.D.; Knadler, M.S. Cellular Properties of Unstable Detonations from Homogeneous and Heterogeneous Mixtures of Two Fuels with Nitrous Oxide. In Proceedings of the AIAA SCITECH 2022 Forum, San Diego, CA, USA, 3–7 January 2022; p. 1750.
24. Pavalavanni, P.K.; Kim, J.E.; Choi, J.-Y. Numerical Investigation of the detonation cell bifurcation with decomposition technique. *Aerospace* **2023**, *10*, 318. [CrossRef]
25. Lu, F.K.; Braun, E.; Massa, L.; Wilson, D. Rotating detonation wave propulsion: Experimental challenges, modeling, and engine concepts (Invited). *AIAA Pap.* **2011**, *6043*, 2011.
26. Wolański, P. Application of the continuous rotating detonation to gas turbine. *Appl. Mech. Mater.* **2015**, *782*, 3–12. [CrossRef]
27. Bedick, C.; Ferguson, D. Quantitative Ion Probe Measurements for Application in a Rotating Detonation Engine. *AIAA J.* **2020**, *58*, 4003–4016. [CrossRef]
28. Han, H.-S.; Lee, E.S.; Choi, J.-Y. Experimental investigation of detonation propagation modes and thrust performance in a small rotating detonation engine using C_2H_4/O_2 propellant. *Energies* **2021**, *14*, 1381. [CrossRef]
29. Qi, L.; Dong, J.; Hong, W.; Wang, M.; Lu, T. Investigation of rotating detonation gas turbine cycle under design and off-design conditions. *Energy* **2023**, *264*, 126212. [CrossRef]
30. Koo, I.-H.; Lee, K.-H.; Kim, M.-S.; Han, H.-S.; Kim, H.; Choi, J.-Y. Effects of Injector Configuration on the Detonation Characteristics and Propulsion Performance of Rotating Detonation Engine (RDE). *Aerospace* **2023**, *10*, 949. [CrossRef]
31. Shi, L.; Shen, H.; Wen, C.-Y.; Shang, S.; Hu, H. Numerical study of the effects of injection conditions on rotating detonation engine propulsive performance. *Aerospace* **2023**, *10*, 879. [CrossRef]
32. Wang, Z.; Yan, C.; Zheng, L.; Fan, W. Experimental study of ignition and detonation initiation in two-phase valveless pulse detonation engines. *Combust. Sci. Technol.* **2009**, *181*, 1310–1325. [CrossRef]
33. Fan, W.; Yan, C.; Huang, X.; Zhang, Q.; Zheng, L. Experimental investigation on two-phase pulse detonation engine. *Combust. Flame* **2003**, *133*, 441–450. [CrossRef]
34. Li, J.-M.; Teo, C.J.; Chang, P.-H.; Li, L.; Lim, K.S.; Khoo, B. Excessively fuel-rich conditions for cold starting of liquid-fuel pulse detonation engines. *J. Propuls. Power* **2017**, *33*, 71–79. [CrossRef]
35. Tan, W.; Zheng, L.; Lu, J.; Wang, L.; Zhou, D. Experimental Investigations on Detonation Initiation Characteristics of a Liquid-Fueled Pulse Detonation Combustor at Different Inlet Air Temperatures. *Energies* **2022**, *15*, 9102. [CrossRef]
36. Gubin, S.A.; Sichel, M. Calculation of the detonation velocity of a mixture of liquid fuel droplets and a gaseous oxidizer. *Combust. Sci. Technol.* **1977**, *17*, 109–117. [CrossRef]
37. Bar-Or, R.; Sichel, M.; Nicholls, J.A. The propagation of cylindrical detonations in monodisperse sprays. *Symp. (Int.) Combust.* **1981**, *18*, 1599–1606. [CrossRef]
38. Kadosh, H.; Michaels, D. Experimental study of pulse detonation engine with liquid ethanol and oxygen mixtures. *Shock Waves* **2022**, *32*, 353–362. [CrossRef]
39. Li, J.-M.; Chang, P.-H.; Li, L.; Yang, Y.; Teo, C.J.; Khoo, B.C. Investigation of injection strategy for liquid-fuel rotating detonation engine. In Proceedings of the 2018 AIAA Aerospace Sciences Meeting, Kissimmee, FL, USA, 8–12 January 2018; p. 0403.
40. Choi, M.H.; Oh, Y.; Park, S. Investigation of spray Characteristics for detonability: A study on Liquid Fuel Injector and Nozzle Design. *Aerospace* **2024**, *11*, 421. [CrossRef]

41. Yan, Y.; Fan, W.; Wang, K.; Zhu, X.-D.; Mu, Y. Experimental investigations on pulse detonation rocket engine with various injectors and nozzles. *Acta Astronaut.* **2011**, *69*, 39–47. [CrossRef]
42. Fickett, W.; Davis, W.C. *Detonation: Theory and Experiment*; Courier Corporation: North Chelmsford, MA, USA, 2000.
43. Guo, D.; Zybin, S.V.; An, Q.; Goddard, W.A., III; Huang, F. Prediction of the Chapman–Jouguet chemical equilibrium state in a detonation wave from first principles based reactive molecular dynamics. *Phys. Chem. Chem. Phys.* **2016**, *18*, 2015–2022. [CrossRef] [PubMed]
44. Gordon, S.; McBride, B.J. *Computer Program for Calculation of Complex Chemical Equilibrium Compositions and Applications. Part 1: Analysis*; NASA: Washington, DC, USA, 1994.
45. Panicker, P.K. The Development and Testing of Pulsed Detonation Engine Ground Demonstrators. Ph.D. Thesis, The University of Texas at Arlington, Arlington, TX, USA, 23 July 2008.